Taylor & Francis
Taylor & Francis Group

Check for updates

Photocatalytic asphalt mixtures: semiconductors' impact in skid resistance and texture

I. Rocha Segundo [a]* , S. Landi Jr. [b,c], S. Oliveira[a], E. Freitas [a], M.F. Costa [b] and J. Carneiro [b]

ᵃCivil Engineering Department, University of Minho, Azurém Campus, Guimarães, Portugal; ᵇCentre of Physics, University of Minho, Azurém Campus, Guimarães, Portugal; ᶜFederal Institute Goiano, Rio Verde – GO, Brazil

Photocatalytic asphalt mixtures have the capability of mitigating air quality problems and degrade oils/greases by using semiconductors. The techniques to do so can change their functional characteristics. This study aimed to analyse the functionalization effect on the essential surface characteristics, such as macrotexture, skid resistance, and microtexture. AC 14 and AC 6 mixtures were functionalised with nano-TiO_2 and micro-ZnO by spraying and bulk incorporation. Mean Profile Depth, British Pendulum and microtexture amplitude parameters were evaluated. TiO_2 application seemed to smooth the surface slightly. In dry condition, the skid resistance of functionalised asphalt and control mixtures was similar. In wet condition, the functionalization caused a maximum decrease of 7% in skid resistance. The amplitude parameters were not affected by any functionalization technique except the skewness of AC 14 with 6% TiO_2 by bulk incorporation. Furthermore, the application of the semiconductors can be used without high impacts in texture and skid resistance.

Keywords: photocatalytic asphalt mixtures; macrotexture; microtexture; skid resistance; optical non-contact rugometric characterisation

Introduction

Functionalization is the development of capabilities for materials, different from the essential ones, usually related to the surface. Implemented by semiconductors, such as TiO_2 and ZnO, photocatalytic and self-cleaning asphalt pavements can decrease the atmospheric concentration of gases NO_x and SO_2, mitigating air pollution (Dylla, Asadi, Hassan, & Mohammad, 2013; Tang, Liu, Huang, & Cao, 2017). Moreover, these materials can, by the self-cleaning property, degrade organic compounds, such as oils and greases, removing them from the surface to have safer roads (Rocha Segundo, Ferreira, et al., 2018). This is possible by the heterogeneous photocatalytic process, which results from the absorption of photons with energy equal to or greater than the band gap of the semiconductor, exciting the electrons, which go from the valence band to the conduction band. This migration generates an electron/hole pair (e^-/h^+). This pair, e^- and h^+, provides oxidation–reduction reactions, forming respectively hydroxyl (HO*) and superoxides (O_2^-) radicals in the presence of water and oxygen molecule. They react with the pollutants presented over the surface, degrading them (Dalton et al., 2002; Heller, 1995).

In general, three approaches have been carried out to develop photocatalytic asphalt pavements: (i) spraying deposition; (ii) bulk incorporation, (iii) bitumen modification (Cao, Yang, Li, Huang, & Liu, 2017; Carneiro et al., 2013; Hassan, Dylla, Asadi, Mohammad, & Cooper, 2012).

---

*Corresponding author. Email: iran_gomes@hotmail.com

There are advantages and disadvantages in each approach depending on the level of wearing (abrasion) by traffic.

The photocatalytic efficiency is much higher for the spraying coating than the functionalization by bulk incorporation before abrasion (Carneiro et al., 2013). After abrasion, the photocatalytic efficiency of sprayed samples is highly reduced, while for bulk incorporation samples it increases with the level of abrasion (Rocha Segundo, Landi Jr., Oliveira, Freitas, & Carneiro, 2018).

Some studies have already addressed the effect of functionalization on mechanical properties. High content of TiO_2 (6%) improved the rutting resistance but decreased fatigue resistance. Conversely, low content of TiO_2 (3%) increased the rutting slightly but maintained the fatigue resistance, as could be expected. Also, by bulk incorporation, TiO_2 leads to a decrease in moisture resistance. By spraying, the application of semiconductors did not cause any deterioration of the mechanical performance (Rocha Segundo, Ferreira, et al., 2018).

As with the mechanical properties, after the application of the semiconductors on asphalt mixtures, the assessment of functional characteristics, such as skid resistance and texture, is very important to assure safety. At least, these characteristics should preserve their current limits. This analysis is not often considered in previous works.

The main functional characteristics, which contribute to safety, comfort and environmental issues, are: tire-road noise, skid resistance, texture (divided in micro, macro, megatexture and roughness), drainability, and rolling resistance (Ejsmont, Ronowski, Świeczko-Żurek, & Sommer, 2017; Li, Wang, & Li, 2016; Noyce, Bahia, Yambó, & Kim, 2005; Praticò & Vaiana, 2015). The texture has a moderate, high and very high influence on the skid resistance, rolling resistance, tire wearing, tire-road noise, drainability, and light reflection, depending on the scale (Li et al., 2016; Noyce et al., 2005).

The evaluation of micro/macrotexture and skid resistance of asphalt mixtures that compose top layers is essential since they are strongly linked to road safety. Microtexture is related to the small-scale texture of the pavement, spatial wavelengths up to 0.5 mm and of amplitudes up to 0.2 mm (controlling the contact between the tire and the surface). This characteristic is provided mainly by the roughness of the aggregates which become polished with traffic loading (Noyce et al., 2005). The microtexture has a very high influence on skid resistance. When the aggregates of the pavement surface get polished due to traffic wearing, the microtexture smoothens, causing the reduction of friction (Wu & Abadie, 2018).

Macrotexture is related to a larger scale texture, wavelengths between 0.5 and 50 mm and amplitude between 0.2 and 10 mm. In this scale, the higher irregularities are related to the voids between aggregates particles, determined by the coarse aggregates' size, shape, and gradation. It is essential for water removal from the pavement surface, avoiding the hydroplaning (Noyce et al., 2005; Wang, Yan, Huang, Chu, & Abdel-Aty, 2011).

Texture characterisation techniques can be grouped into two categories: scale-independent and scale-dependent. The scale-independent parameters are not affected by the measuring scale or data resolution while the scale-dependent parameters are dependent on the scale. The scale-dependent parameters, also called as geometric texture indicators, can be divided into 5 types of categories: (i) amplitude parameters, (ii) functional parameters, (iii) spectral analysis, (iv) spacing parameters and (v) hybrid parameters (Li et al., 2016).

Some amplitude parameters, such as Mean Profile Depth (MPD), Skewness (Ssk), Kurtosis (Sku), Average roughness or Arithmetic Mean Deviation of the Surface (Sa), Root-mean-square Deviation of the Surface (Sq), are used to characterise texture of the asphalt mixtures by 3D measurement (Čelko, Kováč, & Kotek, 2016; Li et al., 2016). Due to the scale, it is difficult to acquire microtexture. However, there are a few types of equipment, such as the optical triangulation based-microtopographer, capable of doing it in asphalt mixtures (Costa, 2012). Previous work carried out with this equipment showed that the amplitude parameters Sa, Sq and Total

Height of the Surface (St) are not directly affected by the type of bitumen (Costa, Freitas, Torres, & Cerezo, 2017).

The skid resistance is the friction force developed at the contact of tire and pavement (Ejsmont et al., 2017; Noyce et al., 2005). Friction has mainly two factors: hysteresis and adhesion. Hysteresis is caused by tire rubber deformations, producing energy dissipation. Adhesion results from the interaction of the shearing of molecular bonds formed when the tire rubber is in contact with pavement surface (Noyce et al., 2005). The skid resistance decreases when pavements are wet, generating the worst contact conditions between the tire and the pavement motivated by the difficulty of water drainage.

Thus, this research aimed to analyse the impact of the semiconductors on functional characteristics, such as skid resistance and texture. For this, two asphalt mixtures AC 6 and AC 14 were evaluated. Both were functionalised by spraying coating and one of them, AC 14, was also functionalised by bulk incorporation. Macrotexture, microtexture and skid resistance tests were carried out.

Materials and methods

Materials

In this research, AC 14 Surf 35/50 and AC 6 Surf Elaster 13/60 asphalt mixtures were evaluated. They are composed of 5% and 6% of binder, respectively. Their mineral composition was:

- AC 6 – limestone filler, 3%; 0/4 mm, 25% and 4/6 mm, 72%;
- AC 14 – limestone filler, 3%; 0/4 mm, 41%; 4/8 mm, 12% and 6/14 mm, 44%.

Both asphalt mixtures were sprayed with TiO_2 and/or ZnO. In the AC 14, TiO_2 was also introduced by bulk incorporation.

Three aqueous solutions were prepared with nano-TiO_2 (4 g/L), micro-ZnO (1 g/L) and the combination of the semiconductors with the same concentration. According to previous work, the pH 8 was kept (Carneiro et al., 2013; Rocha Segundo, Ferreira, et al., 2018; Rocha Segundo, Landi Jr., et al., 2018). Each solution was sprayed over the asphalt mixtures at 60°C, covering 5 mg/cm² to 12.5 mg/cm². In the samples with TiO_2 by bulk incorporation, the limestone filler was partially replaced with 3% and 6% of TiO_2 in mass of the bitumen, resulting in 2.84% and 2.68% of limestone filler respectively (Rocha Segundo, Ferreira, et al., 2018; Rocha Segundo, Landi Jr., et al., 2018).

The designation of the conventional asphalt mixtures was AC 14 and AC 6. For those ones functionalised by bulk incorporation, it was AC 14 3% and AC 14 6% considering the content of TiO_2, 3 and 6%, respectively. Finally, those ones functionalised by spraying coating were called AC 14 TiO_2, AC 14 ZnO, AC 14 TiO_2 ZnO, AC 6 TiO_2, AC 6 ZnO, AC 6 TiO_2 ZnO, considering each treatment over the asphalt mixtures. Table 1 identifies the mixtures selected for this research, how the semiconductors were applied, the Maximum Bulk Density (MBD) and the Void Content (VC) of the mixes.

Methods

The tests selected were skid resistance, microtexture, and macrotexture. Skid resistance and microtexture tests were carried out in all the mixtures. The macrotexture was assessed only in the mixtures without semiconductors and also in the mixtures functionalised by bulk incorporation since the application of the nano/micromaterials by spraying coating does not affect the

Table 1. Properties of asphalt mixes.

Asphalt mix	Semiconductors	Technique	MBD (g/cm^3)	VC (%)
AC 6	TiO$_2$ and/or ZnO	Spraying	2.423	10.9
AC 14	TiO$_2$ and/or ZnO	Spraying	2.426	4.4
AC 14 3%	3% TiO$_2$	Bulk incorporation	2.377	3.8
AC 14 6%	6% TiO$_2$	Bulk incorporation	2.356	4.4

macrotexture due to their very lower scale. All the tests were carried out before any abrasion technique.

Macrotexture

To measure the macrotexture of asphalt mixtures, profiles of the surface were acquired by a device equipped with a laser, and the Mean Profile Depth was calculated. This device allows determining with precision profiles of slabs with a surface of 25×25 cm^2, recording x, y, and z positions. It can acquire profiles every 0.2 mm with a vertical resolution up to 0.01 mm. The MPD was calculated in each profile for a 10 cm baseline. The baseline of the profiles is divided by half of the length, and the average of their two peak heights is used to calculate the MPD (Equation 1).

$$MPD = \frac{1st\,Peak + 2nd\,peak}{2} - average\,level \qquad (1)$$

Skid resistance

To access the skid resistance of the mixtures before and after the application of the semiconductors, Pendulum tests were carried out (EN 13036-4). This test is one of the most popular procedures to determine skid resistance and is widely used to analyse small samples of asphalt mixtures in the laboratory and also highway pavements in some situations. For highways, this test is still used due to the low cost and ease of operation (Asi, 2007).

Microtexture

To measure the microtexture, an optical microtopographer was used. With large measuring range, high versatility, robustness and reliability, good accuracy and resolution, the MICRO-TOP.06.MFC microtopographer (Figure 1) was used to inspect a wide range of surface types (Costa, 2012), including asphalt mixtures (Costa et al., 2017). The system is based on discreet active triangulation. Basically, in this sensor, a beam of light shines on the surface at some angle, and the reflected light is collected at another angle.

The surface is scanned by an oblique light beam. The incident light is collimated and focused. A small, diffraction limited, bright spot is thus projected onto the surface. The bright spot is imaged both perpendicularly and specularly onto electronic photosensitive detection systems to assess its lateral position. The point-by-point scanning of the sample is carried out by the movement of a precision XYZ displacement on a rectangular array separated by distances down to 1.25 μm. By triangulation sensing of the reflected light at each scanning position, a full 3D inspection of the sample is achieved.

Testing set up and analysis

The macrotexture of each mixture was calculated by averaging the MPD of all profiles.
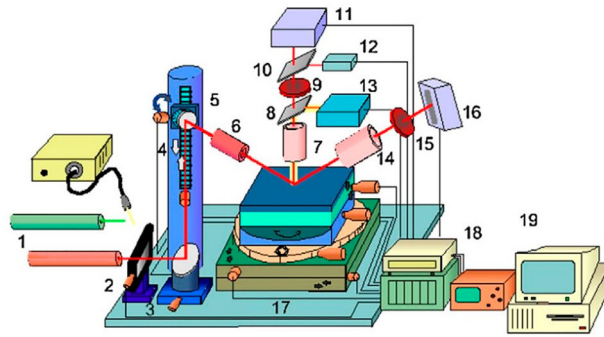
1. Interchangeable light sources; 2. Vibration isolation stand; 3. Neutral density filter; 4. Beam steering system; 5. Incidence angle control motorised system; 6. Incidence optics; 7. Normal observation optics; 8 and 10. Beam splitters; 9. Interference filter; 11. Normal photosensitive detection system; 12. Photodetector; 13. Video camera and illuminator; 14. Specular observation optics; 15. Interference filter; 16. Specular photosensitive detection system; 17. Sample support and motorised positioning system; 18. Data acquisition and control system; 19. Microcomputer

Figure 1.   The MICROTOP.06.MFC (Costa, 2012).

The skid resistance test was carried out in wet and dry conditions at five different temperatures, resulting in 100 Pendulum tests. For the wet procedure, the water and the pavement were conditioned at the same temperature, which made possible the control of the system's temperature. This procedure was carried out to analyse whether the presence of the semiconductors could change skid resistance.

The microtexture of the surfaces of each asphalt mixture slab was acquired in 9 selected squares with $1\,cm^2$. In each square, a silicone cast was applied to have a high-fidelity replica of the microtexture. This material is composed of white liquid silica rubber and a catalyst that allows the hardening in some minutes. Its removal is easy and non-invasive. In total, 90 silicone casts were done to carry out the microtopography measurement within an area of $4\,mm^2$. This procedure was carried out due to the colour of the asphalt mixtures, naturally black, which affects the measurements due to light diffusion during the acquisition. With the use of the white silicone replicas, this measurement problem is prevented since the diffusion of the red light (632.8 nm) into the silicone replica is low (Costa, 2008). Also, it is clean and avoids the placement of large slabs of asphalt mixtures into the device.

The main roughness parameters calculated were: Arithmetic Mean Deviation of the Surface (Sa), Root-mean-square Deviation of the Surface (Sq), Total Height of the Surface (St), Maximum Peak Height of the Surface (Sp), Maximum Valley Depth of the Surface (Sv), Ten-point Height roughness of the Surface (Sz), Skewness (Ssk), Kurtosis (Sku). The parameters Sa and Sq were used to quantify significant deviations of textures. The symmetry of peaks and valleys of the surface about the average surface is established for $Ssk = 0$: normal distribution, that is, symmetry about the average line; $Ssk < 0$: predominance of valleys (negative texture); and $Ssk > 0$: indicates a higher number of peaks (positive texture). The Kurtosis (Sku) characterises the presence of extremely deep valleys/high peaks for $Sku = 3$: normal distribution; $Sku > 3$: extremely deep valleys/high peaks; and $Sku < 3$: lack of them.

These parameters show with detail how texture can change. Therefore, their variation due to the different testing setups was analysed by comparison with reference conditions (samples without treatment).

Analysis of variance (ANOVA), considering as factors mixture and treatment, was carried out to determine whether there was an interaction effect between the independent variables (Sa, Sq, St, Sp, Sv, Sz, Ssk and Sku) over the parameters for a significance level of $(1 - \alpha = 0.1)$.

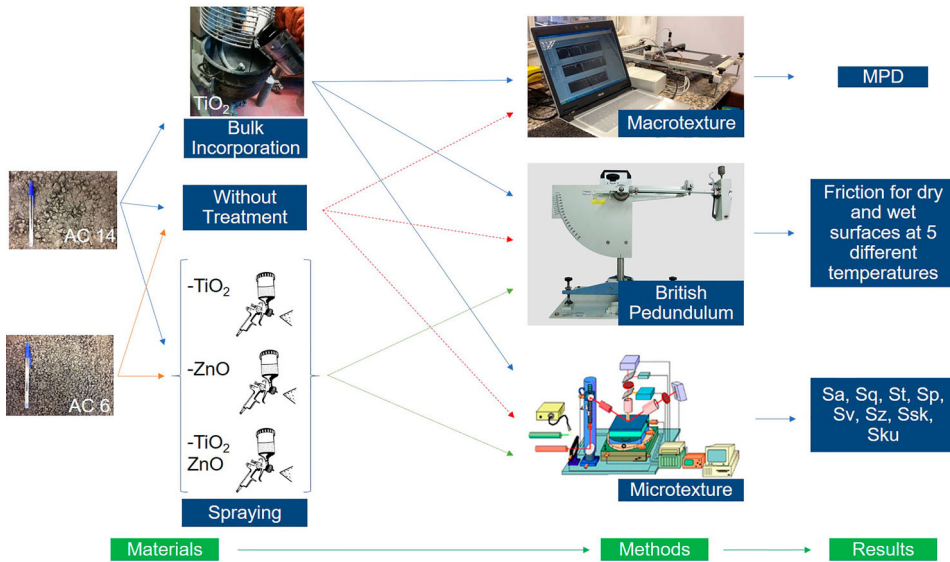Figure 2.   Flow chart of this study.

Table 2.   Macrotexture results.

Mixture	MPD (mm)
AC 6	0.85
AC 14	0.70
AC 14 3%	0.66
AC 14 6%	0.64

Bonferroni Post-Hoc analysis was also carried out to find patterns between subgroups by testing if there was a significant difference in the average of the parameters between samples. Figure 2 shows the flow chart of this study in order to facilitate understanding.

Results

Macrotexture

Table 2 shows the macrotexture results. Explained by their formulation, the AC 6 was 21% rougher than the AC 14. The functionalization by bulk incorporation did not affect the macro-texture of the asphalt mixtures greatly. Both mixtures with TiO_2, independently to the content of nanomaterial, had similar MPD. However, when compared with the control mixture (AC 14), the incorporation of TiO_2 seems to have affected the surface by smoothing it on average 7%.

Skid resistance

Figure 3 shows the skid resistance versus temperature, and Table 3 shows the linear regression fit parameters for each material (results in Pendulum Test Value – PTV).

In dry condition, the skid resistance of functionalised asphalt mixtures was similar to those without treatment. The AC 6 showed PTV values 2% lower than the AC 14, except for the lowest temperature. At the lowest temperature (10°C), the surface got probably wet by water that
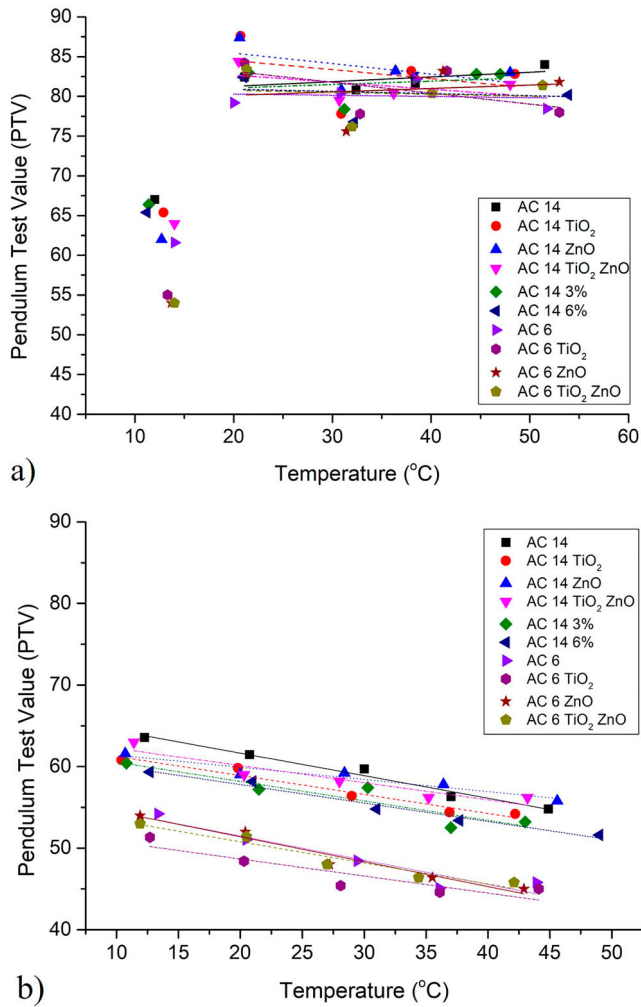
Figure 3.   Results of pendulum test: (a) Dry condition and (b) Wet condition.

condensed during the conditioning procedure, reducing the PTV value to those similar to the wet condition. Due to this, the results of the lowest temperature were removed from the linear trends for the dry condition. Moreover, R^2 values were lower than 0.35, indicating a low sensitivity of PTV to temperature variation.

In wet condition, the application of semiconductors on AC 14 did not have a pronounced impact on skid resistance. Furthermore, the trend lines of the AC 6 almost overlapped, except for AC 6 TiO_2. For both mixtures, after spraying, the minimum and maximum differences in PTV ranged between -6% (TiO_2 at 29°C) and 3% (ZnO at 36°C and TiO_2 ZnO at 43°C). For bulk incorporation, the minimum and maximum differences in PTV were -7% (AC 14 3% at 22°C) and 2% (AC 14 6% at 38°C).

To summarise, for the spraying technique, the maximum absolute difference was 6%, corresponding to a decrease from 48 to 45 PTV. For bulk incorporation, the maximum absolute difference was 7%, corresponding to a decrease from 61 to 57 PTV. The AC 6 mixture had in average a skid resistance 16% lower than the AC 14 mixture. This result indicates that skid

Table 3.   Linear trend equations for skid resistance.

Mixture	Dry Surface		Wet Surface	
	Linear Trend Equation	R^2	Linear Trend Equation	R_2
AC 6	PTV $= -0.015\,T + 80.591$	0.015	PTV $= -0.296\,T + 57.405$	0.907
AC 6 TiO$_2$	PTV $= -0.137\,T + 85.900$	0.302	PTV $= -0.208\,T + 52.838$	0.813
AC 6 ZnO	PTV $= +0.043\,T + 79.261$	0.027	PTV $= -0.305\,T + 57.490$	0.958
AC 6 TiO$_2$ ZnO	PTV $= -0.025\,T + 81.246$	0.011	PTV $= -0.259\,T + 55.974$	0.937
AC 14	PTV $= +0.059\,T + 80.074$	0.302	PTV $= -0.277\,T + 67.182$	0.978
AC 14 TiO$_2$	PTV $= -0.114\,T + 86.779$	0.111	PTV $= -0.233\,T + 63.555$	0.958
AC 14 ZnO	PTV $= -0.132\,T + 88.084$	0.299	PTV $= -0.149\,T + 62.891$	0.921
AC 14 TiO$_2$ ZnO	PTV $= -0.089\,T + 84.458$	0.228	PTV $= -0.211\,T + 64.341$	0.879
AC 14 3%	PTV $= +0.043\,T + 80.189$	0.053	PTV $= -0.238\,T + 62.923$	0.857
AC 14 6%	PTV $= -0.027\,T + 81.439$	0.020	PTV $= -0.193\,T + 61.021$	0.936

Note: PTV = Pendulum Test Value for Skid Resistance; T = temperature (°C).

resistance is higher for mixtures with higher nominal maximum aggregate size, according to results for asphalt concretes (Wang et al., 2011).

A linear trend of PTV and temperature was established with R^2 higher than 0.80, nevertheless lower for the AC 6 mixture. The skid resistance decreased with temperature which is according to literature results for conventional mixtures (Bazlamit & Reza, 2005).

Considering all conditions, the linear trend of PTV and temperature (T) for the AC 14 and AC 6 resulted in Equations 2 and 3 with R^2 equals to 0,766 and 0.833, respectively. The lower slope of the AC 14 (-0.224) compared to the AC 6 (-0.268) shows that AC 6 was more sensitive to temperature. The factor type of surface proved to be important when the pavement was wet. Also, the functionalised mixtures were less sensitive to the temperature than control mixtures, reporting a lower slope, except for AC 6 ZnO.

$$PTV_{AC14} = -0.224T + 63.195 \tag{2}$$

$$PTV_{AC6} = -0.268T + 55.937 \tag{3}$$

In conclusion, there is no change of skid resistance with temperature after the addition of the semiconductors when applied by spraying an aqueous solution or bulk incorporation. AC 6 was less influenced by the semiconductors when sprayed, which may have resulted from the higher porosity of the mixture. Also, either in dry or wet condition, the semiconductors did not cause a high impact in the skid resistance of the asphalt mixtures. This is important since the promotion of the new capacity did not cause a big impact on the most important functional characteristic of the pavement surfaces analysed.

Microtexture

Figure 4 shows the results of the microtexture assessment for the following parameters: Sa, Sq (both related to surface deviations), St (total height of the surface), Sp (maximum peak height of the surface), Sv (maximum valley depth of the surface) and Sz (ten-point height of the surface). In Figure 5 are shown the results of Ssk (symmetry) and Sku (presence of extremely deep valleys/high peaks).

The results of the roughness parameters are characterised by a large dispersion. In general, the results of AC 6 were more dispersed than the ones of AC 14. As the aggregates are smaller for AC 6, it may have influenced the sampling process.
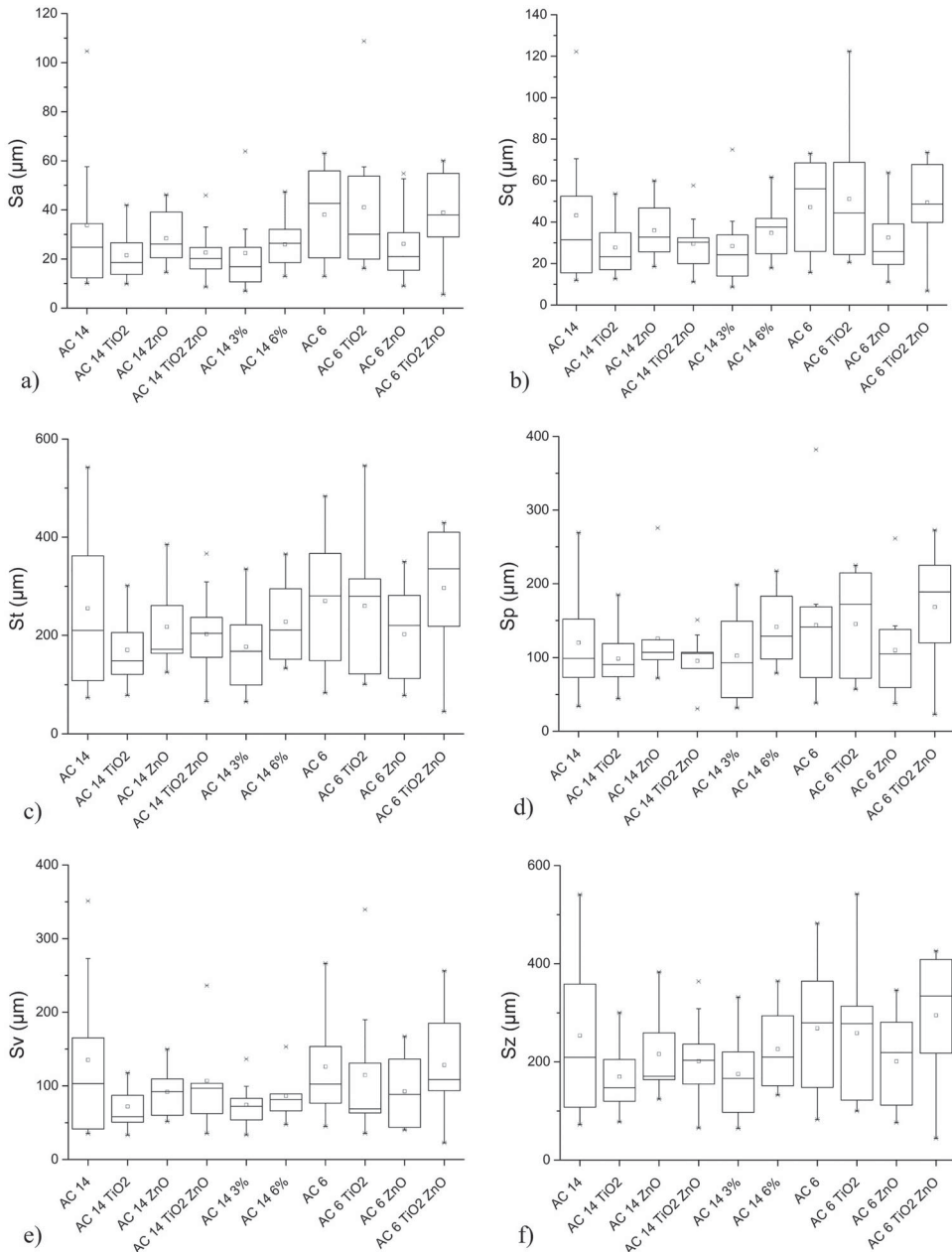
Figure 4.   Microtexture results: (a) Sa, (b) Sq, (c) St, (d) Sp, (e) Sv and (f) Sz.

For symmetry, the results show a normal distribution for most of the materials (Sku = 3, included between the first and third quartiles), except for AC 14 TiO$_2$, AC 14 TiO$_2$ ZnO, and AC 14 6%. These three mixture combinations have the first quartile higher than 3, identifying extremely deep valleys/high peaks. Regarding the skewness (Ssk), the mixtures had the first quartile higher than 0, excluding AC 14 6% and AC 6 TiO$_2$, indicating only positive values, thus all of them conducting to a positive microtexture, and AC 14 6% and AC 6 TiO$_2$, with a negative first quartile and positive third quartile (normal distribution).
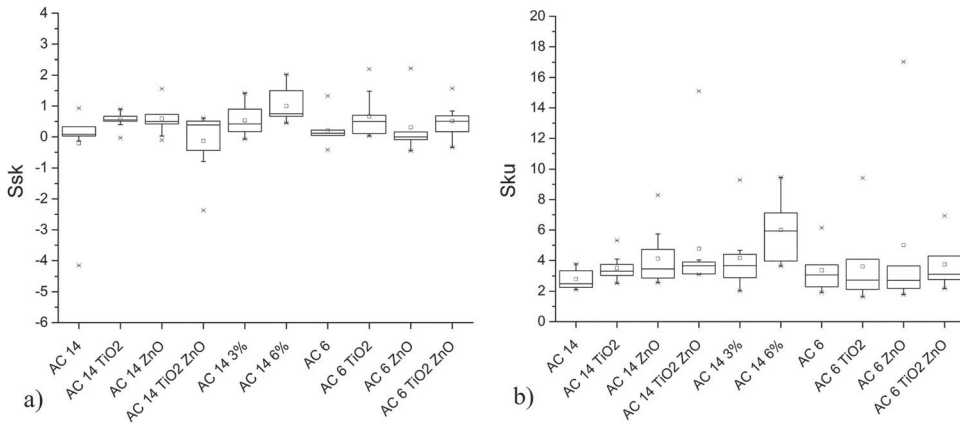
Figure 5.   Microtexture results: (a) Ssk and (b) Sku.

The analysis of the factors influencing the microtexture parameters by ANOVA shows, on the one hand, that the independent variable Mixture had a significant influence on Sa, Sq, Sp, St and Sz ($p < 0.1$). On the other hand, the variable Treatment had a significant effect only on skewness (Ssk). The interaction of Mixture and Treatment variables had no significant effect on the dependent variables results.

The Bonferroni Post-Hoc test for a level of significance ($1 – α = 0.1$) was carried out as well. The averages of Sa, Sq, St, Sp, Sz for the AC 6 samples were significantly higher than for the AC 14 samples ($p < 0.1$). Moreover, AC 6 microtexture deviation was higher ($> Sa$ and Sq) and was characterised by higher total height ($> St$), peaks ($> Sp$), valleys ($> Sv$) and ten-point heights ($> Sz$) than AC 14.

Therefore, the mixture with the smaller aggregate size provided the roughest microtexture. However, it did not correspond to the mixture with the highest skid resistance. This relationship could be a consequence of the larger contact area offered by the AC 14.

For the different treatments, the PostHoc test carried out showed just one difference in the average of the independent variables. The average of the skewness (Ssk) for the AC 14 6% was significantly lower than for the AC 14 ($p < 0.1$).

As final remarks, the asphalt mixture type was a significant factor for the microtexture characterisation, and the functionalization had a low impact in this characteristic.

Conclusions

This research aimed to analyse the skid resistance and the texture of different asphalt mixtures after functionalization by spraying and bulk incorporation. This is one of the first researches contributing to the analysis of the functional characteristics, namely macro/microtexture and skid resistance, of functionalised asphalt mixtures. When new capabilities are developed, it is important to assess these characteristics to guarantee road safety. The results of the experimental activity led to the following conclusions:

- For the macrotexture, the AC 6 was 21% rougher than the AC 14, that bulk incorporation of TiO_2, may have slightly smoothed the surface.
- For skid resistance, in the dry condition, the asphalt mixtures had similar skid resistance independently of the temperature.

- For skid resistance, in wet condition, the surface type and temperature showed to be important factors. AC 6 had a PTV 16% lower than the AC 14 mixture and was also more sensitive to temperature changes, indicating that skid resistance is higher for mixtures with higher nominal maximum aggregate size and lower temperatures.
- Also in wet condition, the functionalization by spraying conducted to a difference in PTV between -6% (TiO_2 at 29°C) and 3% (ZnO at 36°C and TiO_2 ZnO at 43°C). By bulk incorporation, this interval was between -7% (AC 14 3% at 22°C) and 2% (AC 14 6% at 38°C). Therefore, the maximum absolute difference was 7%, corresponding to a decrease of 4 PTV.
- For microtexture, only Sa, Sq, Sp, St, and Sz had a significant influence the asphalt from the mixture type with significantly higher averages for the AC 6. AC 6 also had more dispersed microtexture, higher peaks and ten-point heights than AC 14. It can be justified by the microtexture assessment for AC 14, which was carried out also over fine aggregates bonded with a binder, conducting to a smoother surface. Only the average of the parameter Ssk of the AC 14 6% was significantly lower than the AC 14 samples ($p < 0.1$).

In conclusion, in general, the treatments did not affect the amplitude parameters of microtexture. Thereby, the functionalization had a low impact on skid resistance and texture, allowing the application of the semiconductors by bulk incorporation and spraying. Road safety is in this way assured for the study conditions.

Although the goals of this research were achieved, it is important to carry out this kind of analysis in more and larger samples to allow, since the microtexture is a very small surface area and skid resistance could be measured with other techniques. In addition, the next step of this research is the assessment of texture and skid resistance after abrasion techniques.

Disclosure statement

Funding

ORCID

I. Rocha Segundo http://orcid.org/0000-0002-4199-5994
S. Landi Jr. http://orcid.org/0000-0003-1830-7548
E. Freitas http://orcid.org/0000-0001-5132-7407
M.F. Costa http://orcid.org/0000-0002-1554-8779
J. Carneiro http://orcid.org/0000-0001-9778-5390

References

Asi, I. M. (2007). Evaluating skid resistance of different asphalt concrete mixes. *Building and Environment*, *42*(1), 325–329. doi:10.1016/j.buildenv.2005.08.020
Bazlamit, S. M., & Reza, F. (2005). Changes in asphalt pavement friction components and adjustment of skid number for temperature. *Journal of Transportation Engineering*, *131*(6), 470–476. doi:10.1061/(ASCE)0733-947X(2005)131:6(470)

Cao, X., Yang, X., Li, H., Huang, W., & Liu, X. (2017). Investigation of Ce-TiO_2 photocatalyst and its application in asphalt- based specimens for NO degradation. *Construction and Building Materials*, *148*, 824–832. doi:10.1016/j.conbuildmat.2017.05.095

Carneiro, J. O. O., Azevedo, S., Teixeira, V., Fernandes, F., Freitas, E., Silva, H., & Oliveira, J. (2013). Development of photocatalytic asphalt mixtures by the deposition and volumetric incorporation of TiO_2 nanoparticles. *Construction and Building Materials*, *38*, 594–601. doi:10.1016/j.conbuildmat.2012.09.005

Čelko, J., Kováč, M., & Kotek, P. (2016). Analysis of the pavement surface texture by 3D scanner. *Transportation Research Procedia*, *14*, 2994–3003. doi:10.1016/j.trpro.2016.05.434

Costa, M. F. M. (2008). *Microtopographical characterization of microcavities on X-rays sensor array*. In *AIP Conference Proceedings* (pp. 507–512). doi:10.1063/1.2926840

Costa, M. F. M. (2012). Optical triangulation-based microtopographic inspection of surfaces. *Sensors*, *12*(4), 4399–4420. doi:10.3390/s120404399

Costa, M. F. M., Freitas, E. F., Torres, H., & Cerezo, V. (2017). Optical microtopographic inspection of asphalt pavement surfaces. *Proceedings of SPIE - The International Society for Optical Engineering*, *10453*. doi:10.1117/12.2270880

Dalton, J. S., Janes, P. A., Jones, N. G., Nicholson, J. A., Hallam, K. R., & Allen, G. C. (2002). Photocatalytic oxidation of NO_x gases using TiO_2: A surface spectroscopic approach. *Environmental Pollution*, *120*(2), 415–422. doi:10.1016/S0269-7491(02)00107-0

Dylla, H., Asadi, S., Hassan, M., & Mohammad, L. N. (2013). Evaluating photocatalytic asphalt pavement effectiveness in real-world environments through developing models: A statistical and kinetic study. *Road Materials and Pavement Design*, *14*(sup2), 92–105. doi:10.1080/14680629.2013.812839

Ejsmont, J. A., Ronowski, G., Świeczko-Żurek, B., & Sommer, S. (2017). Road texture influence on tyre rolling resistance. *Road Materials and Pavement Design*, *18*(1), 181–198. doi:10.1080/14680629.2016.1160835

Hassan, M. M., Dylla, H., Asadi, S., Mohammad, L. N., & Cooper, S. (2012). Laboratory evaluation of environmental performance of photocatalytic titanium dioxide warm-mix asphalt pavements. *Journal of Materials in Civil Engineering*, *24*(5), 599–605. doi:10.1061/(ASCE)MT.1943-5533.0000408

Heller, A. (1995). Chemistry and applications of photocatalytic oxidation of thin organic films. *Accounts of Chemical Research*, *28*(12), 503–508. doi:10.1021/ar00060a006

Li, L., Wang, K. C. P., & Li, Q. "Joshua." (2016). Geometric texture indicators for safety on AC pavements with 1 mm 3D laser texture data. *International Journal of Pavement Research and Technology*, *9*(1), 49–62. doi:10.1016/j.ijprt.2016.01.004

Noyce, D. A., Bahia, H. U., Yambó, J. M., & Kim, G. (2005). *Incorporating Road Safety into Pavement Management: Maximizing Asphalt Pavement Surface Friction for Road Safety Improvements*. *Draft Literature Review and State Surveys*. Madison, USA.

Praticò, F. G., & Vaiana, R. (2015). A study on the relationship between mean texture depth and mean profile depth of asphalt pavements. *Construction and Building Materials*, *101*, 72–79. doi:10.1016/j.conbuildmat.2015.10.021

Rocha Segundo, I., Ferreira, C., Freitas, E. F., Carneiro, J. O., Fernandes, F., Landi Júnior, S., & Costa, M. F. (2018). Assessment of photocatalytic, superhydrophobic and self-cleaning properties on hot mix asphalts coated with TiO_2 and/or ZnO aqueous solutions. *Construction and Building Materials*, *166*, 36–44. doi:10.1016/j.conbuildmat.2018.01.106

Rocha Segundo, I., Landi Jr, S., Oliveira, S. M. B., Freitas, E. F. d., & Carneiro, J. A. O. (2018, July). Photocatalytic asphalt mixtures: Mechanical performance and impacts of traffic and weathering abrasion on photocatalytic efficiency. *Catalysis Today*. doi:10.1016/j.cattod.2018.07.012

Tang, B., Liu, X., Huang, W., & Cao, X. (2017). Preparation of La-doped nanometer TiO_2 and its application for NO removal on asphalt concrete. *Road Materials and Pavement Design*, *18*(S3), 43–53. doi:10.1080/14680629.2017.1329860

Wang, W., Yan, X., Huang, H., Chu, X., & Abdel-Aty, M. (2011). Design and verification of a laser based device for pavement macrotexture measurement. *Transportation Research Part C: Emerging Technologies*, *19*(4), 682–694. doi:10.1016/j.trc.2010.12.001

Wu, Z., & Abadie, C. (2018). Laboratory and field evaluation of asphalt pavement surface friction resistance. *Frontiers of Structural and Civil Engineering*, *12*(3), 372–381.